Soft Matter

PAPER

View Article Online
View Journal | View Issue

Cite this: *Soft Matter*, 2018, **14**, 5856

Emergent magnetoelectricity in soft materials, instability, and wireless energy harvesting

Zeinab Alameh,†[a] Shengyou Yang,†[a] Qian Deng[b] and Pradeep Sharma *[ac]

Received 21st March 2018,
Accepted 21st May 2018

DOI: 10.1039/c8sm00587g

rsc.li/soft-matter-journal

Magnetoelectric materials that convert magnetic fields into electricity and *vice versa* are rare and usually complex, hard crystalline alloys. Recent work has shown that soft, highly deformable magnetoelectric materials may be created by using a strain-mediated mechanism. The electromagnetic and elastic deformation of such materials is intricately coupled, giving rise to a rather rich instability and bifurcation behavior that may limit or otherwise put bounds on the emergent magnetoelectric behavior. In this work, we investigate the magneto-electro-mechanical instability of a soft dielectric film subject to mechanical forces and external electric and magnetic fields. We explore the interplay between mechanical strain, electric voltage and magnetic fields and their impact on the maximum voltage and the stretch the dielectric material can reach. Specifically, we present physical insights to support the prospects to achieve wireless energy harvesting through remotely applied magnetic fields.

1 Introduction

Soft materials that are capable of undergoing large mechanical deformation in response to external stimuli (such as temperature, pH or electric field) have recently received extensive attention. As example, soft dielectrics respond to electric fields and have been investigated for applications in human-like robots,[1,2] stretchable electronics,[3] actuators[4–6] and energy harvesting.[7–11] Magnetoelectric coupling refers to the ability of the materials to electrically polarize under the application of a magnetic field, and conversely, magnetize under the application of an electric field. Unfortunately, there are no known natural soft magnetoelectric materials. Magnetoelectricity was discovered in a class of hard, crystalline multiferroics.[12–14] The intrinsic coupling is low at room temperature and these materials can hardly sustain large deformations.‡

Soft materials that are magnetoelectric are expected to have several interesting applications such as wireless energy transfer,[17] spintronics and nonvolatile memories,[18] multiple state energy bits that can be written electrically and retrieved magnetically, among others.[14] Perhaps the most enticing one is that of wireless energy harvesting. Magnetic fields may be remotely imposed and therefore a suitable magnetoelectric soft material may provide a facile route to convert magnetic power into electric energy. Coupled with the large-deformation capability of soft materials, these materials present a compelling case as actuators, sensors and energy conversion devices. In recent works, a rather simple approach to create artificial soft magnetoelectric materials was proposed by Liu, Sharma and co-workers[19–21] that does not require the materials themselves to be magnetoelectric, or piezoelectric or exhibit any exotic atomistic features that conventional hard crystalline multiferroics do. Rather, any soft material may be made to act like a magnetoelectric material (Fig. 1) provided certain conditions are met.

For instance, a soft dielectric film coated with two compliant electrodes under an applied voltage will deform because of the electric Maxwell stress—and this deformation is proportional to the square of the applied electric field. What will happen to the dielectric response if an external magnetic field is applied in addition to the applied voltage? If the dielectric material also has a magnetic permeability larger than unity, then it will deform further due to the magnetic Maxwell stress. The superimposed additional deformation will, in turn, alter the pre-existing electric field and thus, change the polarization (see Fig. 1). The detectable change in the electric field resulting from the application of the magnetic field manifests itself as a magnetoelectric effect.[19,20] Since the aforementioned mechanism relies mainly on electric and magnetic Maxwell stress the resulting magnetoelectric effect is universal. Here, we note

[a] *Department of Mechanical Engineering, University of Houston, Houston, TX 77204, USA*
[b] *State Key Laboratory for Strength and Vibration of Mechanical Structures, School of Aerospace, Xi'an Jiaotong University, Xi'an, Shaanxi, 710049, P. R. China*
[c] *Department of Physics, University of Houston, Houston, TX 77204, USA. E-mail: psharma@uh.edu; Fax: +1-713-743-4503; Tel: +1-713-743-4502*
† These authors contributed equally to this paper.

‡ An alternative approach to artificially design hard composite magnetoelectric materials is by combining piezoelectric and magnetostrictive materials. Most such resulting materials are also hard, the ensuing coupling is not strong and suffers from challenges related to cost-effectiveness and the associated complex fabrication processes.[15,16]

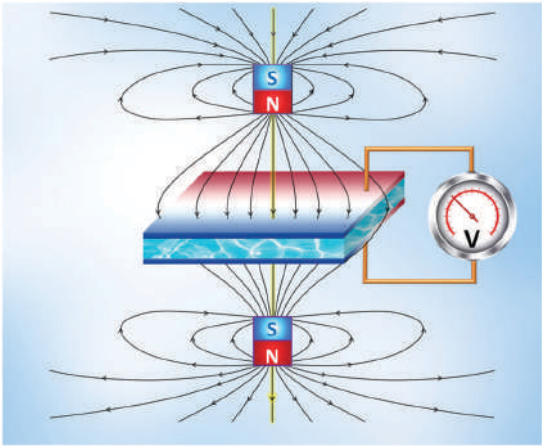

Fig. 1 Schematic figure illustrating the mechanism that can be used to engineer the magnetoelectric effect in soft materials. A thin film made of an elastically soft material is coated with two compliant electrodes. When subjected to a pre-existing electric potential, the dielectric will be deformed and be polarized by the electric field. Now, if an external magnetic field is switched on, the magnetic Maxwell stress will also deform the thin film if its magnetic permeability $\mu_r > 1$. That, in turn, alters the existing polarization and deformation. The change in the polarization in the film can be measured as a current due to the imposed magnetic field and thus manifests as an emergent strain-mediated magnetoelectric effect.

three essential conditions for the effect to take place.[19–21] First, the material must be mechanically soft so that the electrical Maxwell stress effect is significant. Second, the dielectric material must have a magnetic permeability larger than that of vacuum. That is, the magnetic permeability of the soft material must be greater than one, $\mu_r > 1$. The latter can be ensured by incorporating a very minute amount of soft magnetic particles or fluid.[22] Finally, a pre-existing electric field must be present.

A large deformation in soft matter and instabilities go hand-in-hand. For example, soft dielectrics are vulnerable to a wide range of electro-mechanical instabilities including thinning and pull-in instabilities,[23–25] electro-creasing to cratering,[26] electro-cavitation,[27] wrinkling to name just a few.[28,29] Historically, instabilities have been considered harmful (and they indeed can be) but more recently, especially in the context of soft dielectrics, they have also been exploited to enhance material behavior and design novel devices.[30] While the literature on the discussion of instability in dielectrics (and its avoidance or enhancement) is extensive, very few works have focussed on analogous issues in the context of soft magnetically responsive materials.[22,31–33] In this work, (i) we analyze the magneto-electro-mechanical stability of a soft dielectric film subjected to a combination of mechanical, electrical and magnetic stimuli, (ii) present insights into the resulting phenomenon of strain-mediated magnetoelectricity, and (iii) explore the prospects for wireless energy harvesting due to remotely applied magnetic fields.

The outline of this work is as follows: in Section 2, we present the theoretical formulation, first in general terms and then specialized for the thin-film configuration of interest which we use to illustrate our key results. In Section 3 we specialize our derivations to homogeneous deformation and for an ideal dielectric elastomer. We present the central results related to stability and the magnetoelectric effect in Section 4 and discuss wireless energy harvesting in Section 5. Finally, we conclude our work in Section 6.

2 Formulation

In this section, we derive the governing equations needed to investigate the magneto-electromechanical stability of soft dielectric materials subjected to a combination of mechanical forces and external electric and magnetic fields. We assume the simplest possible configuration: a film of soft material sandwiched between two electrodes (see Fig. 2). This will facilitate exploration of the key mechanisms and insights underpinning magnetoelectricity in soft materials while avoiding excessive mathematical tedium. The material forming the layer is assumed to be elastically nonlinear but electrostatically and magnetostatically linear.

2.1 Geometry and deformation

If we consider a film of soft dielectric and choose a positively-oriented, orthonormal basis $\{\mathbf{e}_X, \mathbf{e}_Y, \mathbf{e}_Z\}$ with associated Cartesian coordinates X, Y, and Z, the domain occupied by the dielectric film (see Fig. 2), in the reference configuration, is given by

$$\mathscr{B} = \{\mathbf{X} \in \mathbb{R}^3 : 0 \leq X \leq L_1,\ 0 \leq Y \leq L_2,\ 0 \leq Z \leq L_3\}, \qquad (1)$$

where L_i, $i = 1, 2, 3$, are geometrical dimensions.

The deformation is denoted by a smooth mapping: χ: $\mathscr{B} \to \mathbb{R}^3$ and the deformed film dimensions become (l_1, l_2, l_3). In contrast to the material point $\mathbf{X} \in \mathscr{B}$, the spatial point is then represented by $\mathbf{x} = \chi(\mathbf{X})$, which is denoted by the Cartesian triplet (x, y, z) in the current configuration.

We consider the following class of deformations

$$x = X + a(X), \quad y = Y(1 + b(X)), \quad z = Z(1 + c(X)), \qquad (2)$$

where $a(X)$, $b(X)$ and $c(X)$ are functions of only the variable X.

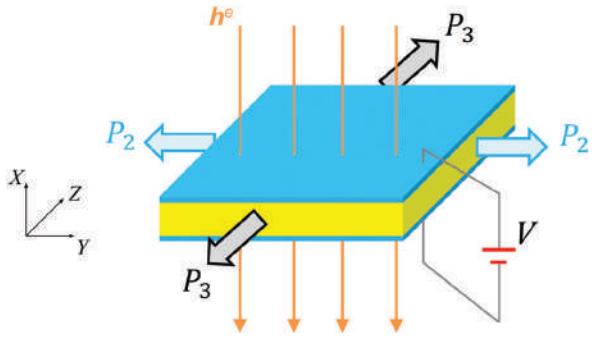

Fig. 2 A film of soft dielectric material subject to two pairs of in-plane mechanical loads P_2 and P_3, an applied electrical voltage difference V between the upper and bottom surfaces coated with compliant electrodes, and an external magnetic field h^e in the thickness direction.

The deformation gradient is

$$\mathbf{F} = \frac{\partial \chi}{\partial \mathbf{X}} = \begin{pmatrix} \lambda_1 & 0 & 0 \\ Yb'(X) & \lambda_2 & 0 \\ Zc'(X) & 0 & \lambda_3 \end{pmatrix}, \tag{3}$$

where the prime denotes the derivative with respect to X and the stretches§ are

$$\lambda_1 = \frac{\partial x}{\partial X} = 1 + a'(X), \tag{4a}$$

$$\lambda_2 = \frac{\partial y}{\partial Y} = 1 + b(X), \tag{4b}$$

and

$$\lambda_3 = \frac{\partial z}{\partial Z} = 1 + c(X). \tag{4c}$$

The (volumetric) Jacobian then becomes

$$J = \det \mathbf{F} = \lambda_1\lambda_2\lambda_3, \tag{5}$$

where λ_i is given in (4). For incompressible materials, the Jacobian in (5) is unity

$$J = 1 \tag{6}$$

and then the stretches have the relation

$$\lambda_1 = \frac{1}{\lambda_2\lambda_3}. \tag{7}$$

2.2 Maxwell's equations and boundary conditions

2.2.1 Maxwell's equations. In the current configuration, the Maxwell equations are[20,34]

$$\operatorname{div}(-\varepsilon_0 \operatorname{grad} \xi + \mathbf{p}) = 0, \quad \operatorname{div}(-\operatorname{grad} \zeta + \mathbf{m}) = 0, \tag{8}$$

where ε_0 is the vacuum permittivity, "div" and "grad" are the divergence and gradient operators, ξ is the electric potential field and ζ is the magnetic potential field. **p** and **m**, respectively, denote the polarization and the magnetization.

The relations between the polarization and the magnetization in the current and reference configurations are[19,20,34]

$$\mathbf{p} = \frac{\mathbf{P}}{J}, \quad \mathbf{m} = \frac{\mathbf{M}}{J}, \tag{9}$$

where **P** and **M**, respectively, denote the polarization and the magnetization in the reference configuration. Other definitions of these relations between the true and the nominal polarization (or magnetization), see for example the definition by Dorfmann and Ogden,[35] can also be used if the expressions of the corresponding Maxwell equations are properly articulated. The current choice of the defined nominal magnetization in (9) is consistent with our formulation.

2.2.2 Electric and magnetic boundary conditions. The electric boundary conditions on the upper ($x = l_1$) and bottom ($x = 0$) surfaces in the current configuration are

$$\xi|_{x=l_1} = V, \quad \xi|_{x=0} = 0, \tag{10}$$

where x is the coordinate in the current configuration and l_1 is the thickness of the deformed film.

The far-field magnetic boundary condition is[20,34]

$$-\operatorname{grad} \zeta \to \mathbf{h}^{\mathrm{e}} \quad \text{as } |\mathbf{x}| \to \infty, \tag{11}$$

where **x** is the spatial point and $\mathbf{h}^{\mathrm{e}} = h^{\mathrm{e}}\mathbf{e}_x$ is the external far-field magnetic field in the current configuration with basis $\{\mathbf{e}_x, \mathbf{e}_y, \mathbf{e}_z\}$.

From Ampère's law for time-independent problems and in the absence of external currents, we have the following interface discontinuity/boundary condition for the magnetic field on the upper ($x = l_1$) and bottom ($x = 0$) surfaces

$$\mathbf{n} \times [\![-\operatorname{grad} \zeta]\!] = \mathbf{0} \quad \text{on } x = 0 \ \& \ l_1, \tag{12}$$

where **n** is a unit normal to the surface and $[\![f]\!] = f_+ - f_-$, is the difference of the field quantity f evaluated at either side of the discontinuity surface.

In addition, given the absence of "magnetic monopoles" at the interfaces, we have the following interface discontinuity/boundary condition for the magnetic flux:

$$\mathbf{n} \cdot [\![-\mu \operatorname{grad} \zeta]\!] = \mathbf{0} \quad \text{on } x = 0 \ \& \ l_1, \tag{13}$$

where μ is the magnetic permeability.

2.3 Free energy of the system

The total free energy of a general conservative magneto-electro-mechanical system in a three-dimensional space can be expressed as[34]

$$\mathscr{F}[\chi,\mathbf{P},\mathbf{M}] = \mathscr{U}[\chi,\mathbf{P},\mathbf{M}] + \mathscr{E}^{\mathrm{elect}}[\chi,\mathbf{P}] + \mathscr{E}^{\mathrm{mag}}[\chi,\mathbf{M}] + \mathscr{P}^{\mathrm{mech}}[\chi]. \tag{14}$$

Here, $\mathscr{U}$ is the internal energy

$$\mathscr{U} = \int_{\mathscr{B}} W(\chi, \mathbf{P}, \mathbf{M}), \tag{15}$$

where $\mathscr{B}$ is the domain of the system in the reference configuration and $W(\chi,\mathbf{P},\mathbf{M})$ is the internal energy function. The smooth function χ: $\mathscr{B} \to \mathscr{B}^\star$ that is assigned to each material point $\mathbf{X} \in \mathscr{B}$ a spatial point $\mathbf{x} \in \mathscr{B}^\star$.

In addition, $\mathscr{E}^{\mathrm{elect}}$ in (14) is the electric energy

$$\mathscr{E}^{\mathrm{elect}} = \frac{\varepsilon_0}{2}\int_{\mathscr{B}^\star} |\operatorname{grad}\xi|^2 + \int_{\partial\mathscr{B}_{\mathrm{d}}^\star} \xi(-\varepsilon_0 \operatorname{grad} \xi + \mathbf{p}) \cdot \mathbf{n}, \tag{16}$$

where $\mathscr{B}^\star$ is the domain of the deformed body and $\partial\mathscr{B}_{\mathrm{d}}^\star$ is the electric boundary in the current configuration, and **n** is the unit normal to the surface $\partial\mathscr{B}_{\mathrm{d}}^\star$.$\mathscr{E}^{\mathrm{mag}}$ in (14) is the magnetic energy¶

$$\mathscr{E}^{\mathrm{mag}} = \frac{\mu_0}{2}\int_{\mathbb{R}^3} |\operatorname{grad}\zeta|^2 = \frac{\mu_0}{2}\int_{\mathbb{R}^3} |\operatorname{grad}\zeta^{\mathrm{self}}|^2 - \mu_0\int_{\mathscr{B}^\star} \mathbf{h}^{\mathrm{e}} \cdot \mathbf{m}, \tag{17}$$

where μ_0 is the magnetic permeability of free space, $\mathbf{h}^{\mathrm{e}}$ is the far-field applied magnetic field and **m** is the magnetization in the current configuration. ζ^{self} is the so-called magnetic self-field which is defined for convenience by decomposing

§ The stretches here are not the principal stretches of the deformation.

¶ The detailed derivation of the form of the magnetic energy and the expression of (17) can be found in eqn (5.1)–(5.5) of the work by Liu.[34]

the total magnetic field $\mathbf{h}$ as: $\mathbf{h} = \mathbf{h}^{\mathrm{e}} + \mathbf{h}^{\mathrm{self}}$ and $\mathbf{h}^{\mathrm{self}} = -\mathrm{grad}\,\zeta^{\mathrm{self}}$ and $\mathbf{h} = -\mathrm{grad}\,\zeta$. Finally, $\mathscr{P}^{\mathrm{mech}}$ in (14) is defined by

$$\mathscr{P}^{\mathrm{mech}} = -\int_{\partial\mathscr{B}_t} \mathbf{t}\cdot\chi \tag{18}$$

that is the potential energy related to the dead load $\mathbf{t}$ applied on the traction boundary $\partial\mathscr{B}_t$.

In this work, we will consider the case of a dielectric elastomer subject to two in-plane biaxial forces P_2 and P_3, an applied voltage (10) and an external far-field magnetic field (11) in the thickness direction (see Fig. 2). Considering the assumption of the deformation (see eqn (2)–(7)) and the 1-dimensional nature of the problem, the total free energy of the system shown in Fig. 2, in contrast to the general form (14) in the three-dimensional space, is given by[19,20]

$$\begin{aligned}\frac{F}{L_1L_2L_3} &= \frac{1}{L_1}\int_0^{L_1} W(\lambda_2,\lambda_3,P,M)\mathrm{d}X + \frac{1}{L_1}\int_0^{l_1}\frac{\varepsilon_0}{2}\lambda_2\lambda_3(\xi_{,x})^2\mathrm{d}x\\ &\quad+\frac{1}{L_1}\left[\xi\lambda_2\lambda_3(-\varepsilon_0\xi_{,x}+p)\right]\big|_{x=l_1}\\ &\quad+\frac{1}{L_1}\int_0^{l_1}\frac{\mu_0}{2}\lambda_2\lambda_3(\zeta^{\mathrm{self}}_{,x})^2\mathrm{d}x\\ &\quad-\frac{1}{L_1}\int_0^{l_1}\lambda_2\lambda_3\mu_0\mathbf{h}^{\mathrm{e}}\cdot\mathbf{m}\mathrm{d}x-\frac{P_2\lambda_2}{L_1L_3}-\frac{P_3\lambda_3}{L_1L_2},\end{aligned} \tag{19}$$

where the subscript '$,x$' denotes the derivative with respect to x in the current configuration.

The free energy expression (19) contains a mixture of both material and spatial representations. In the following subsection, we will reformulate the free energy expression entirely in the reference configuration.

2.3.1 Material representation of the free energy. Recalling the expression for the stretch λ_1 in (4), the relationship between the differentials in the current and reference configurations can be written as

$$\xi_{,x} = \xi_{,X}\frac{\partial X}{\partial x} = \frac{\xi_{,X}}{\lambda_1},\quad \zeta^{\mathrm{self}}_{,x} = \frac{\zeta^{\mathrm{self}}_{,X}}{\lambda_1},\quad \mathrm{d}x = \lambda_1\mathrm{d}X. \tag{20}$$

In contrast to the spatial forms (8), the 1D Maxwell equations in the reference configuration are

$$(-\varepsilon_0\lambda_2\lambda_3\xi_{,X}+P)_{,X} = 0,\quad (-\lambda_2\lambda_3\zeta_{,X}+M)_{,X} = 0. \tag{21}$$

Thus the free energy (19) can be written in the reference configuration as

$$\begin{aligned}\frac{F}{L_1L_2L_3} &= \frac{1}{L_1}\int_0^{L_1} W\mathrm{d}X + \frac{1}{L_1}\int_0^{L_1}\frac{\varepsilon_0}{2}(\lambda_2\lambda_3)^2(\xi_{,X})^2\mathrm{d}X\\ &\quad+\frac{1}{L_1}\int_0^{L_1}\left[-\varepsilon_0(\lambda_2\lambda_3)^2(\xi_{,X})^2+\lambda_2\lambda_3\xi_{,X}P\right]\mathrm{d}X\\ &\quad+\frac{1}{L_1}\int_0^{L_1}\frac{\mu_0}{2}(\lambda_2\lambda_3)^2(\zeta^{\mathrm{self}}_{,X})^2\mathrm{d}X\\ &\quad-\frac{1}{L_1}\int_0^{L_1}\mu_0h^{\mathrm{e}}M\mathrm{d}X-\frac{P_2\lambda_2}{L_1L_3}-\frac{P_3\lambda_3}{L_1L_2}\end{aligned} \tag{22}$$

by using eqn (20), (7), and the 1D Maxwell eqn (21) as well as integration by parts.

2.3.2 A vector form of the free energy. There are four generalized coordinates (independent variables) including λ_2, λ_3, P and M in the expression of the free energy (22). Other variables like the electric potential ξ, the magnetic potential ζ and the self-magnetic potential ζ^{self} are related to the four generalized coordinates through relation (20) and Maxwell eqn (21).

By introducing a vector

$$\mathbf{v} = (\lambda_2,\ \lambda_3,\ P,\ M)^T, \tag{23}$$

A more compact form of the free energy (22) can be written as:

$$\frac{F(\mathbf{v})}{L_1L_2L_3} = \frac{1}{L_1}\int_0^{L_1} W^t(\mathbf{v})\mathrm{d}X - s_2\lambda_2 - s_3\lambda_3, \tag{24}$$

where the total energy density $W^t(\mathbf{v})$ is

$$\begin{aligned}W^t(\mathbf{v}) &= W(\mathbf{v}) - \frac{\varepsilon_0}{2}(\lambda_2\lambda_3)^2(\xi_{,X})^2 + \lambda_2\lambda_3\xi_{,X}P\\ &\quad+\frac{\mu_0}{2}(\lambda_2\lambda_3)^2(\zeta^{\mathrm{self}}_{,X})^2 - \mu_0h^{\mathrm{e}}M,\end{aligned} \tag{25}$$

and the nominal stresses are

$$s_2 = \frac{P_2}{L_1L_3},\quad s_3 = \frac{P_3}{L_1L_2}. \tag{26}$$

It should be noted that $\xi_{,X}$ and $\zeta^{\mathrm{self}}_{,X}$ in the energy function (25) are implicitly related to the vector $\mathbf{v}$ in (23).

2.4 Principle of minimum free energy

The equilibrium state $\mathbf{v}$ in (24) is dictated by the principle of minimum free energy. The free energy should be minimized among all the neighboring states $\mathbf{v}+\delta\mathbf{v}$, $|\delta\mathbf{v}| \ll 1$:

$$F(\mathbf{v}) \le F(\mathbf{v}+\delta\mathbf{v}). \tag{27}$$

The inequality (27) gives the following conditions for the first and second variations:

$$\delta F(\mathbf{v}) = 0 \tag{28}$$

and

$$\delta^2F(\mathbf{v}) \ge 0. \tag{29}$$

Using (28) and (29), the first variation condition can be written as:

$$\frac{\delta F}{L_1L_2L_3} = \frac{1}{L_1}\int_0^{L_1}\delta W^t(\mathbf{v})\mathrm{d}X - s_2\delta\lambda_2 - s_3\delta\lambda_3 = 0 \tag{30}$$

while the second variation condition is an integral inequality, such that

$$\frac{\delta^2F}{L_1L_2L_3} = \frac{1}{L_1}\int_0^{L_1}\delta^2W^t(\mathbf{v})\mathrm{d}X \ge 0. \tag{31}$$

We remark that the first and second variations are integral quantities since we have allowed for inhomogeneous states. For homogeneous deformation and perturbation, the Hessian matrix approach is often directly used to study stability.[11,25]

Detailed derivations of the first and second variations can be found in Appendix A.

3 Homogeneous deformation of ideal dielectric elastomers

3.1 Homogeneous deformation

In order to make the calculation simpler and obtain clear insights into our stated objective, we now limit our attention to the homogeneous deformation. That is, the deformation gradient is constant everywhere in the deformed body. This assumption has been used quite frequently to study electromechanical instability.[7,11,25]

For homogeneous deformation of incompressible materials, the deformation gradient (3) reduces to

$$\mathbf{F} = \begin{pmatrix} 1/\lambda_2\lambda_3 & 0 & 0 \\ 0 & \lambda_2 & 0 \\ 0 & 0 & \lambda_3 \end{pmatrix}, \tag{32}$$

where λ_1, λ_2, and λ_3 are undetermined constants that are independent of the coordinates.

In addition, the free energy (24) reduces to

$$\frac{F}{L_1L_2L_3} = W^t(\mathbf{v}) - s_2\lambda_2 - s_3\lambda_3, \tag{33}$$

the first variation condition (30) becomes

$$\frac{\delta F}{L_1L_2L_3} = \frac{\partial W^t}{\partial \mathbf{v}}\cdot\delta\mathbf{v} - s_2\delta\lambda_2 - s_3\delta\lambda_3 = 0 \tag{34}$$

and the second variation condition (31) reads

$$\frac{\delta^2 F}{L_1L_2L_3} = \delta^2 W^t(\mathbf{v}) = \delta\mathbf{v}\cdot\frac{\partial^2 W^t}{\partial \mathbf{v}^2}\delta\mathbf{v} = \delta\mathbf{v}\cdot\mathbb{H}\delta\mathbf{v} \geq 0. \tag{35}$$

This stability condition $\delta^2 F \geq 0$ only requires a positive-definite (Hessian) matrix $\mathbb{H} = \dfrac{\partial^2 W^t}{\partial \mathbf{v}^2}$ at equilibrium.

3.2 Ideal dielectric elastomer

The formulation in the preceding sub-sections is applicable for any soft dielectric material with the internal energy $W(\mathbf{v})$. To produce specific results, we will make a choice of constitutive law and consider an ideal dielectric material[19,20,34]

$$W = \frac{c}{2}(\lambda_2^2 + \lambda_3^2 + \lambda_2^{-2}\lambda_3^{-2} - 3) + \frac{P^2}{2\varepsilon_0(\hat{\varepsilon}_\mathrm{r} - 1)} + \frac{\mu_0 M^2}{2(\hat{\mu}_\mathrm{r} - 1)}, \tag{36}$$

where c is the small-strain shear modulus, and $\hat{\varepsilon}_\mathrm{r}$ and $\hat{\mu}_\mathrm{r}$ are the relative electric permittivity and magnetic permeability of the film, respectively.

The first term in (36) denotes the mechanical part, while the second and third terms are the electric and magnetic parts of the internal energy, respectively. In the absence of electric and magnetic fields, the internal energy simply represents an incompressible neo-Hookean elastic material.

3.3 Equilibrium solutions

With (A.69) and (34), the Euler–Lagrange equations are

$$\frac{\partial W^t}{\partial \lambda_2} - s_2 = 0, \quad \frac{\partial W^t}{\partial \lambda_3} - s_3 = 0, \quad \frac{\partial W^t}{\partial P} = 0, \quad \frac{\partial W^t}{\partial M} = 0. \tag{37}$$

Together with the energy function (36), we have

$$c(\lambda_2 - \lambda_2^{-3}\lambda_3^{-2}) - \varepsilon_0\lambda_2\lambda_3^2(\xi_{,X})^2 + \lambda_3\xi_{,X}P + \mu_0\lambda_2\lambda_3^2(\zeta^{\mathrm{self}}_{,X})^2 - s_2 = 0, \tag{38a}$$

$$c(\lambda_3 - \lambda_2^{-2}\lambda_3^{-3}) - \varepsilon_0\lambda_2^2\lambda_3(\xi_{,X})^2 + \lambda_2\xi_{,X}P + \mu_0\lambda_2^2\lambda_3(\zeta^{\mathrm{self}}_{,X})^2 - s_3 = 0, \tag{38b}$$

$$\frac{P}{\varepsilon_0(\hat{\varepsilon}_\mathrm{r} - 1)} + \lambda_2\lambda_3\xi_{,X} = 0, \tag{38c}$$

$$\frac{\mu_0 M}{(\hat{\mu}_\mathrm{r} - 1)} + \mu_0(\lambda_2\lambda_3)^2\zeta^{\mathrm{self}}_{,X}[\zeta^{\mathrm{self}}_{,X}]_{,M} - \mu_0 h^\mathrm{e} = 0. \tag{38d}$$

In this set of four algebraic equations, we have four unknown independent variables, λ_2, λ_3, P and M. The remaining two variables $\xi_{,X}$ and $\zeta^{\mathrm{self}}_{,X}$ are related to these four independent variables through relation (20) and Maxwell eqn (21). Together with the electric and magnetic boundary conditions, we can solve this set of algebraic equations. In the following, we give the details of the solution.

3.3.1 Solution of the polarization and the electric field. From (38c), we can easily obtain the polarization P in the reference configuration as

$$P = -\varepsilon_0(\hat{\varepsilon}_\mathrm{r} - 1)\lambda_2\lambda_3\xi_{,X}. \tag{39}$$

With (7), (9) and (20), the polarization can be written in the current configuration as

$$p = -\varepsilon_0(\hat{\varepsilon}_\mathrm{r} - 1)\xi_{,x}, \tag{40}$$

which is consistent with the constitutive relation stated earlier in this work.

Substituting (40) into the Maxwell eqn (8), we can obtain a Laplace equation of the electric potential ξ. Together with the electric boundary condition (10), the solution of the potential in the current configuration is given by

$$\xi = \frac{V}{l_1}x, \quad 0 \leq x \leq l_1. \tag{41}$$

Then the electric fields in the current and reference configurations are

$$-\xi_{,x} = -\frac{V}{l_1} \tag{42}$$

and

$$-\xi_{,X} = -\lambda_1\xi_{,x} = -\frac{V}{L_1}. \tag{43}$$

For further discussion, we define the magnitude of the nominal electric field as:

$$\tilde{E} = \frac{V}{L_1}. \tag{44}$$

3.3.2 Solution of the magnetization and the magnetic field. Similar to the polarization, from (38d), we can get the magnetization M in the reference configuration as

$$M = (\hat{\mu}_r - 1)(-\lambda_2\lambda_3\zeta^{self}_{,X} + h^e). \tag{45}$$

With (7), (9) and (20), the magnetization in the current configuration is

$$m = (\hat{\mu}_r - 1)(-\zeta^{self}_{,x} + h^e) = -(\hat{\mu}_r - 1)\zeta_{,x}, \tag{46}$$

which, as expected, agrees with our constitutive relation.

Substituting (46) into the Maxwell eqn (8), we have a Laplace equation of the potential ζ. Together with the magnetic boundary conditions (11)–(13), the solution of the magnetic field in the current configuration is given by

$$-\zeta_{,x} = \begin{cases} \dfrac{1}{\hat{\mu}_r}h^e, & 0 < x < l_1, \\ h^e, & \text{otherwise.} \end{cases} \tag{47}$$

Then the magnetization and the self-magnetic field in the current configuration are given by

$$m = \begin{cases} \tilde{h}, & 0 < x < l_1, \\ \hat{\mu}_r\tilde{h}, & \text{otherwise,} \end{cases} \tag{48}$$

and

$$-\zeta^{self}_{,x} = \begin{cases} -\tilde{h}, & 0 < x < l_1, \\ 0, & \text{otherwise,} \end{cases} \tag{49}$$

where

$$\tilde{h} = \frac{(\hat{\mu}_r - 1)}{\hat{\mu}_r}h^e. \tag{50}$$

Using relation (20), the magnetic field, the magnetization and the self-magnetic field in the reference configuration are

$$-\zeta_{,X} = \frac{-\zeta_{,x}}{\lambda_2\lambda_3}, \quad M = m \quad \text{and} \quad -\zeta^{self}_{,X} = \frac{-\zeta^{self}_{,x}}{\lambda_2\lambda_3}. \tag{51}$$

3.3.3 Solution for the stretches. By substituting (39), (43) and (51) into (38a) and (38b), we have

$$c(\lambda_2 - \lambda_2^{-3}\lambda_3^{-2}) - \varepsilon_0\hat{\varepsilon}_r\lambda_2\lambda_3^2\tilde{E}^2 + \mu_0\lambda_2^{-1}\tilde{h}^2 - s_2 = 0, \tag{52}$$

$$c(\lambda_3 - \lambda_2^{-2}\lambda_3^{-3}) - \varepsilon_0\hat{\varepsilon}_r\lambda_2^2\lambda_3\tilde{E}^2 + \mu_0\lambda_3^{-1}\tilde{h}^2 - s_3 = 0. \tag{53}$$

For the sake of convenience, we introduce the following dimensionless variables by appropriate normalization

$$\bar{s}_2 = \frac{s_2}{c}, \quad \bar{s}_3 = \frac{s_3}{c}, \quad E = \tilde{E}\sqrt{\frac{\varepsilon_0\hat{\varepsilon}_r}{c}}, \quad H = \tilde{h}\sqrt{\frac{\mu_0}{c}}. \tag{54}$$

Then (52) and (53) can be recast as

$$(\lambda_2 - \lambda_2^{-3}\lambda_3^{-2}) - \lambda_2\lambda_3^2E^2 + \lambda_2^{-1}H^2 - \bar{s}_2 = 0, \tag{55}$$

$$(\lambda_3 - \lambda_2^{-2}\lambda_3^{-3}) - \lambda_2^2\lambda_3E^2 + \lambda_3^{-1}H^2 - \bar{s}_3 = 0. \tag{56}$$

For given values of control parameters (the dead loads $\bar{s}_2$, $\bar{s}_3$, the electric field E and the magnetic field H) defined in (54), the two equilibrium eqn (55) and (56) determine the values of the two stretches λ_2 and λ_3.

3.4 Stability analysis

According to the principle of minimum energy (27), a homogeneously deformed dielectric will be stable under small perturbations in control parameters when the Hessian matrix $\mathbb{H}$ in (A.74) is positive-definite. By substituting the energy function (36) into the Hessian matrix (A.74), we obtain:

$$\mathbb{H} = \begin{pmatrix} \mathbb{H}_{11} & \mathbb{H}_{12} & \mathbb{H}_{13} & \mathbb{H}_{14} \\ & \mathbb{H}_{22} & \mathbb{H}_{23} & \mathbb{H}_{24} \\ & & \mathbb{H}_{33} & \mathbb{H}_{34} \\ & \text{Sym} & & \mathbb{H}_{44} \end{pmatrix}, \tag{57}$$

where the entries, at the equilibrium solutions (39), (43), (45), and (49)–(56), are

$$\mathbb{H}_{11} = c(1 + 3\lambda_2^{-4}\lambda_3^{-2}) - \varepsilon_0\lambda_3^2\tilde{E}^2 + \mu_0\lambda_2^{-2}\tilde{h}^2, \tag{58a}$$

$$\mathbb{H}_{12} = 2c\lambda_2^{-3}\lambda_3^{-3} - \varepsilon_0(\hat{\varepsilon}_r + 1)\lambda_2\lambda_3\tilde{E}^2 + 2\mu_0\lambda_2^{-1}\lambda_3^{-1}\tilde{h}^2, \tag{58b}$$

$$\mathbb{H}_{13} = \lambda_3\tilde{E}, \tag{58c}$$

$$\mathbb{H}_{14} = 2\mu_0\lambda_2^{-1}\tilde{h}, \tag{58d}$$

$$\mathbb{H}_{22} = c(1 + 3\lambda_2^{-2}\lambda_3^{-4}) - \varepsilon_0\lambda_2^2\tilde{E}^2 + \mu_0\lambda_3^{-2}\tilde{h}^2, \tag{58e}$$

$$\mathbb{H}_{23} = \lambda_2\tilde{E}, \tag{58f}$$

$$\mathbb{H}_{24} = 2\mu_0\lambda_3^{-1}\tilde{h}, \tag{58g}$$

$$\mathbb{H}_{33} = \frac{1}{\varepsilon_0(\hat{\varepsilon}_r - 1)}, \tag{58h}$$

$$\mathbb{H}_{34} = 0, \tag{58i}$$

$$\mathbb{H}_{44} = \frac{\mu_0\hat{\mu}_r}{\hat{\mu}_r - 1}. \tag{58j}$$

In what follows we will limit our discussion to the determinant of the Hessian matrix rather than all its principal minors. For prescribed dead loads P_2 and P_3 and external magnetic field h^e, for example, changing the voltage V takes the system from a state of stable equilibrium to a critical state specified by the condition:

$$\det(\mathbb{H}) = 0. \tag{59}$$

Beyond that, the determinant of the Hessian matrix becomes negative and the equilibrium states are no longer stable.

4 Stability and emergent magnetoelectricity

4.1 In the absence of external magnetic field

To connect with past work on dielectric elastomers, we first consider the scenario when magnetic fields are absent. For $H = 0$, the equilibrium eqn (55) and (56) reduce to

$$(\lambda_2 - \lambda_2^{-3}\lambda_3^{-2}) - \lambda_2\lambda_3^2E^2 - \bar{s}_2 = 0, \qquad (60)$$

$$(\lambda_3 - \lambda_2^{-2}\lambda_3^{-3}) - \lambda_2^2\lambda_3E^2 - \bar{s}_3 = 0. \qquad (61)$$

These two equations are equivalent to eqn (6a) and (6b) in the work of Zhao and Suo[25] with an appropriate change in notation. We remark that the state variables used in the work[25] are the stretch and the nominal electric displacement $\tilde{D}$ while in this paper we have chosen to use the stretch and the nominal polarization P. The connection between various flavors of electromagnetic theories of deformable media has been discussed at length by Liu.[34]

4.2 Effect of the magnetic field on the equilibrium

In this section, we investigate the effect of an external magnetic field. For simplicity of presentation, we consider the special case of equal biaxial stresses, such that $\bar{s}_2 = \bar{s}_3 = S$ in the equilibrium eqn (55) and (56). As a result, $\lambda_2 = \lambda_3 = \lambda$ and the two equilibrium equations become:

$$(\lambda - \lambda^{-5}) - \lambda^3E^2 + \lambda^{-1}H^2 - S = 0, \qquad (62)$$

where the dimensionless electric and magnetic fields E and H are defined by (54). The dimensionless magnetic field H is related to the magnetic parameter $\tilde{h}$ in (50). It is important to note that the magnetic permeability should be $\mu_r = \hat{\mu}_r\mu_0 > \mu_0$ for the emergent magnetoelectric effect to manifest. Therefore, $\tilde{h} = (\hat{\mu}_r - 1)h^e/\hat{\mu}_r > 0$ and $H > 0$ are chosen in our numerical plots of the equilibrium (62) and the stability (57). Note that S, E and H are control parameters that result in the stretch λ. In the absence of the magnetic field, $H = 0$, (62) will yield eqn $(8)_2$ in the work of Zhao and Suo.[25]

For the material properties suggested in ref. 25 the shear modulus of soft dielectric is $c = 10^6$ N m^{-2}, the material permittivity is $\varepsilon_0\hat{\varepsilon}_r = 4 \times 10^{-11}$ F m^{-1}, and the nominal electric field is of the order $\tilde{E} = 10^8$ V m^{-1}. Then the dimensionless electric E in (54) is $E = 0.63$. For a dimensionless magnetic field $H = 0.5$ in (54), we need to input an external magnetic field $\tilde{h} = 0.55$ T (tesla), where $\tilde{h} \approx h^e$ for a large relative magnetic permeability. This external magnetic field can decrease the true electric field from 1.25×10^8 V m^{-1} ($E = 0.63$ and $H = 0$) to 1.07×10^8 V m^{-1} ($E = 0.63$ and $H = 0.5$), which can avoid the electric breakdown of soft dielectrics in some circumstances.

In Fig. 3, we show the stretch λ and the actuation stretch λ/λ^{Ps} of the dielectric film subject to an applied voltage and various dead loads in the absence of a magnetic field. For simplicity, only the case of non-negative E in (62) is plotted. Fig. 3(a) shows that the nominal electric field E increases nonmonotonically with the increase of the in-plane stretch λ under an equal-biaxial load S. Alternatively, the electric field

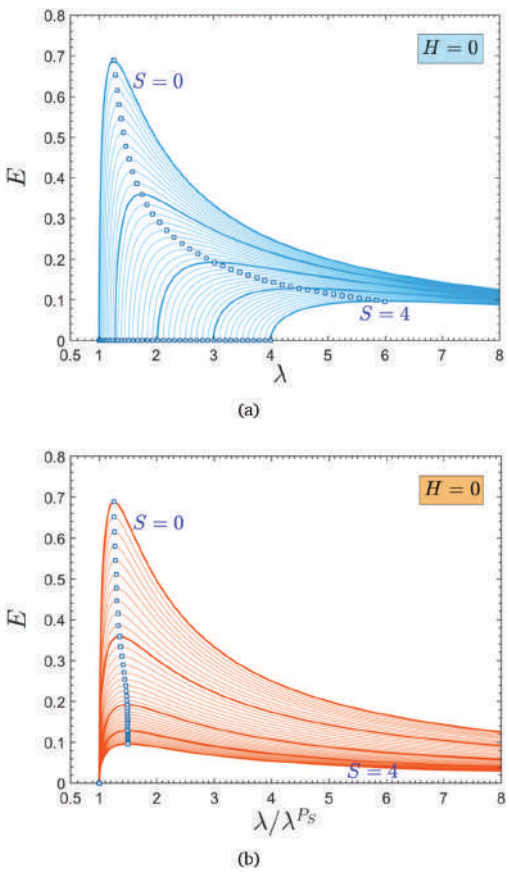

Fig. 3 Behavior of a neo-Hookean dielectric film subjected to a zero magnetic field $H = 0$ under various equal-biaxial loads from $S = 0$ to $S = 4$ in equilibrium: (a) in-plane stretch λ *vs.* nominal electric field E, (b) in-plane actuation stretch λ/λ^{Ps} *vs.* nominal electric field E.

and the dead load can increase the in-plane stretch, that is, they can expand the dielectric film. At a zero electric field $E = 0$, the higher the dead load S, the larger the stretch λ.

For every value of the dead load S, there exists a peak that corresponds to the maximum of the nominal electric field in equilibrium. The maximum E in each curve decreases with the increase of the dead load S and the peak moves from a low stretch (the left) to a high stretch (the right). A point in each curve corresponds to an equilibrium state whose stability can be verified by the positive-definiteness of the Hessian matrix (57). The peak of each curve corresponds to $\det(\mathbb{H}) = 0$, each point on the left-hand side corresponds to a positive-definite Hessian (stable), each point on the right-hand side corresponds to a non-positive-definite Hessian (unstable).

Fig. 3(b) shows how the nominal electric field E affects the actuation stretch. The actuation stretch here is defined as the ratio of the stretch λ to the prestretch λ^{Ps} that is only induced by the dead load. Each curve in Fig. 3(b) starts at the unit actuation stretch and a zero electric field, and then the trend and the stability of each curve are similar to those in Fig. 3(a). These results are to be expected and simply presented as benchmark.

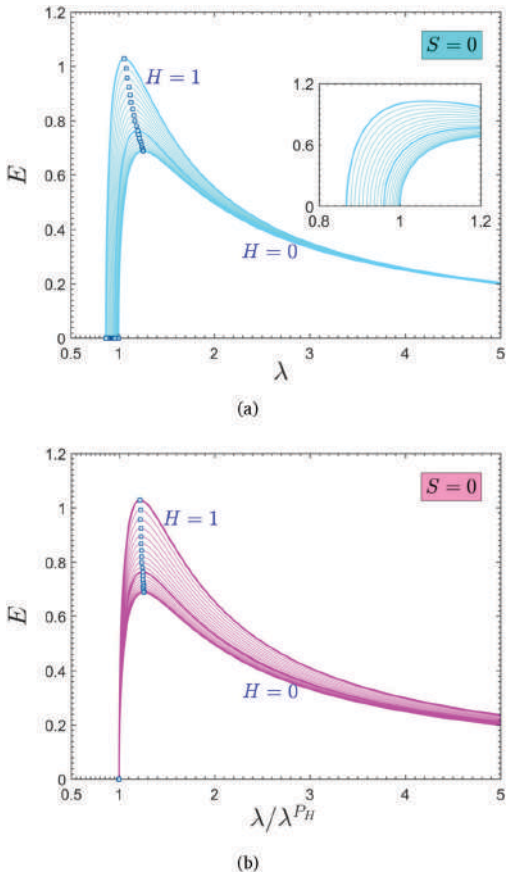

Fig. 4 Behavior of a neo-Hookean dielectric film at a zero dead load $S = 0$ under various magnetic fields from $H = 0$ to $H = 1$ in equilibrium: (a) in-plane stretch λ *vs.* nominal electric field E, (b) in-plane actuation stretch λ/λ^{P_S} *vs.* nominal electric field E.

For detailed discussion of these non-magnetic behaviors, the reader can refer to the work.[7,11,25]

In Fig. 4, we present the stretch λ and the actuation stretch λ/λ^{P_H} of the dielectric film subject to an applied voltage and various magnetic fields. For simplicity, all these curves are plotted at a zero dead load $S = 0$. In Fig. 4(a), with the increase of the magnetic field from $H = 0$ to 1, the peak in each curve increases significantly and moves slightly from a high stretch (the right) to a low stretch (the left). These changes indicate that the magnetic field increases the critical electrical field (the electric field at the peak of each curve). However, the shift of the peak (from right to left) due to the increase of H in Fig. 4(a) is opposite to that observed in Fig. 3(a) (from left to right) resulting from the increase in S. This indicates that the magnetic field squeezes the dielectric film and then decreases the in-plane stretch. Indeed, the magnetic field H has an opposite effect on the in-plane stretch λ compared to the electric field E and the dead load S. The magnetic field compresses the film in-plane while the electric field and the dead load expand it. At a zero electric field $E = 0$, for example, increasing the magnetic field H changes the stretch λ from 1 (at $H = 0$) to 0.87 (at $H = 1$).

The prestretch λ^{P_H}, in contrast to λ^{P_S} in Fig. 3(b), is defined as the stretch induced solely by the magnetic field. Then the actuation stretch by the electric field here is defined as the ratio λ/λ^{P_H}. Unlike the maximum electric field, the actuation stretch of the peak on each curve is insensitive to the increase of the magnetic field.

From the previous discussion of Fig. 3, we know that the magnetic field squeezes the dielectric film in-plane. Since the film is incompressible, the thickness of the dielectric film will increase.

Fig. 5 shows the stretch $\lambda_1 = 1/\lambda^2$ and the actuation stretch $\lambda_1/\lambda_1^{P_H}$ in the thickness direction of the film. To make a direct comparison between the electric and magnetic fields, we choose a zero dead load here. In Fig. 5(a), at a zero electric field $E = 0$, the magnetic field H can increase the thickness from an initial stretch of 1 (at $H = 0$) to a stretch of 1.32 (at $H = 1$). With the increase of the electric field, there exists an apparent competition between the electric and magnetic fields. At a low electric field but a relatively high magnetic field, the stretch is

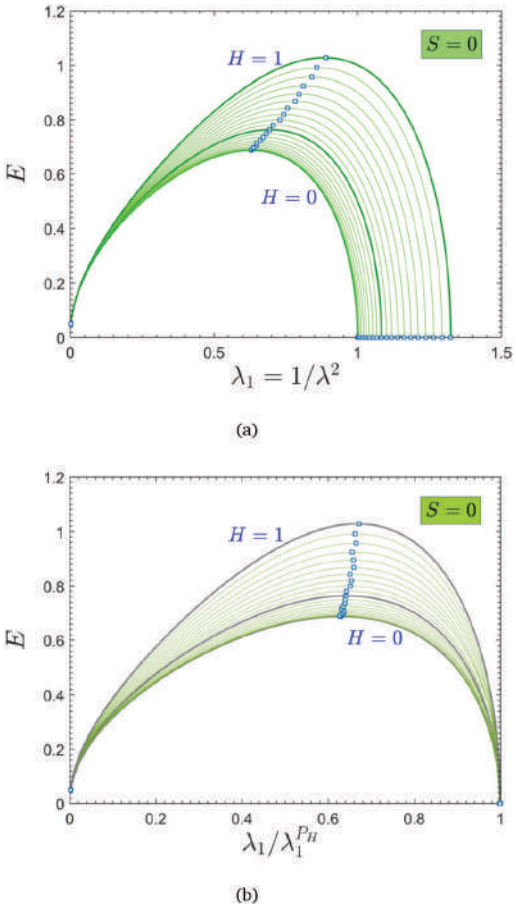

Fig. 5 Behavior of a neo-Hookean dielectric film at a zero dead load $S = 0$ under various magnetic fields from $H = 0$ to $H = 1$ in equilibrium: (a) in-thickness stretch $\lambda_1 = 1/\lambda^2$ *vs.* nominal electric field E, (b) in-thickness actuation stretch $\lambda_1/\lambda_1^{P_H}$ *vs.* nominal electric field E.

greater than one (increasing thickness); at a high electric field but a relatively low magnetic field, the stretch is less than one (decreasing thickness). It is worth mentioning that each point in Fig. 5 on the left-hand side of the peak corresponds to a non-positive-definite Hessian (unstable) while each point on the right-hand side corresponds to a positive-definite Hessian (stable), unlike Fig. 3 and 4.

In Fig. 5(b), the actuation stretch in the thickness direction is plotted. Note that the actuation stretch induced by the electric field compresses the film in the thickness direction. Thus the actuation stretch is always less than 1 in Fig. 5(b) but greater than 1 in Fig. 4(b).

In Fig. 3–5, we examine the effect of a varying nominal electric field (the vertical axis) while fixing the external magnetic field and the dead load on the in-plane and in-thickness stretches (the horizontal axis). The electric and magnetic fields have opposite effects on the in-plane and in-thickness stretches. To further investigate the role of magnetic field, we plot the variation of the in-plane stretch as a result of a varying magnetic field (the vertical axis) at constant nominal electric field and dead load. The results are shown in Fig. 6 for a zero dead load for simplicity. We first note that the plot is symmetric about the horizontal axis. This is expected mathematically because the magnetic field appears as a squared term in the equilibrium eqn (62) which makes it independent of the sign. From a physical point of view, the Maxwell stress is a quadratic form of the magnetic field, and thus the equilibrium state is the same regardless of the magnetic field direction. In addition, for a prescribed nominal electric field E, the equilibrium eqn (62) yields two curves. For an E less than the critical value, between 0.6 and 0.7, the two equilibrium curves are separated on the left and on the right. On the other hand, for an E greater than the critical E, the two equilibrium curves are separated on the top and bottom. In each curve, there exists a turning point. For the up (down) curves, the turning point denotes a minimum (maximum) of the magnetic field; for the left (right) curves, it denotes the maximum (minimum) of the in-plane stretch. Note that a point in each curve corresponds to an equilibrium state and the stability can be verified by the positive definite of the Hessian matrix.

In what follows, we will show that if a point on each curve is on the left-hand side of the turning point, the Hessian is positive-definite and the point stands for a stable equilibrium state. In contrast, if the point is on the right-hand side of the turning point, it denotes an unstable equilibrium state. Therefore, the curve on the left-hand is always stable while the curve on the right-hand side is unstable. For up and down curves, the parts on the left-hand of the turning points are stable, and the right part is unstable.

4.3 Effects of the magnetic field on stability

Each curve in Fig. 3–5 reveals a maximum which corresponds to $\det(\mathbb{H}) = 0$. To further illustrate the magneto-electro-mechanical stability, we consider the sign of the determinant $\det(\mathbb{H})$ of an uniaxial stretched thin film subject to electric and magnetic fields in equilibrium.

Fig. 7 shows the regions of stability and instability for a film of soft materials subject to a uniaxial tension s_1 and a constant electric field under various external magnetic fields. We plot three curves and each of them corresponds to the zero determinant $\det(\mathbb{H}) = 0$ at a given value of the magnetic field, $H = 0$, 0.3, 0.5. For a given H, the curve in Fig. 7 represents the variation of the critical electric field $\tilde{E}^c$ at which $\det(\mathbb{H}) = 0$ with respect to the applied dead load. The determinant is positive (stable) below the curve while it is negative (unstable) above the curve.

It is clear from Fig. 7 that the external magnetic field enhances the magneto-electro-mechanical stability. The curve with a higher magnetic field H is always above the curve with a

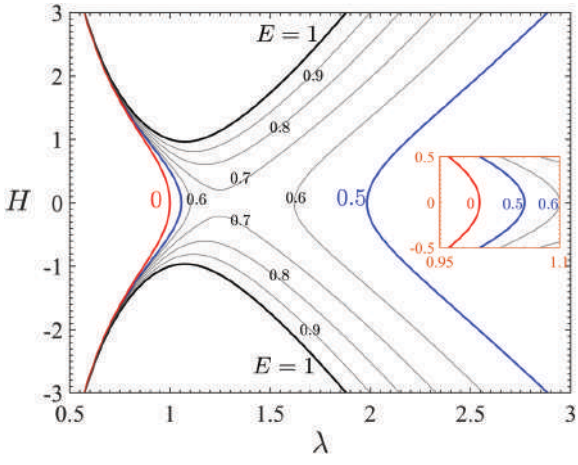

Fig. 6 Behavior of a neo-Hookean dielectric film at a zero dead load $S = 0$ under various nominal electric fields from $E = 0$ to $E = 1$ in equilibrium: in-plane stretch λ *vs.* magnetic field H.

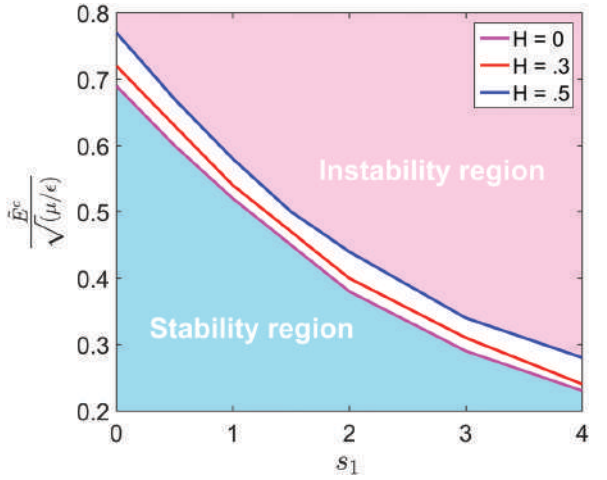

Fig. 7 Stability and instability regions in the dead load (s_1)—electric field plane of a neo-Hookean dielectric film under various magnetic fields $H = 0$, 0.3, 0.5. The stability region is enclosed by the curve of zero determinant and the axes. A higher magnetic field corresponds to a larger stability region.

lower H. Without considering the magnetic field $H = 0$, the curve would be the lowest. A higher curve means a larger stability region that is enclosed by the curve of zero determinant and the axes. This clearly shows that the magnetic field allows the film to sustain a higher electric field. We remark that the electric breakdown is not taken into account here.

5 Wireless actuation and energy harvesting

A key insight evident from the discussion in the preceding paragraphs is that the presence of external magnetic field increases the critical nominal electric field and reduces the critical actuation stretch, thus suppressing pull-in instability. The critical value of the nominal electric field corresponds to the intersection point of the three stresses acting on the dielectric material: the mechanical stress, the electric Maxwell stress and the magnetic Maxwell stress. At a constant external magnetic field, the latter attempts to "squeeze" the material, thus reducing its actuation stretch and increasing its thickness. Changing the external voltage while maintaining constant external magnetic field and mechanical stress will affect the nominal electric field, thus changing the electric Maxwell stress. Since magnetic stress acts against the electric and the mechanical stresses, the material is able to withstand a larger critical electric field, but the critical actuation stretch will be smaller and depends on the magnitude of the magnetic field. Beyond that critical point, any small perturbation will move the film to an unstable state where it fails without reaching an equilibrium. The same effect can be seen in the case of a uniaxial stress (see Fig. 7); the presence of the magnetic field also reduces the actuation stretch and increases the critical electric field as can be seen in Fig. 4 and 5.

We have shown that the applied electric voltage and the external magnetic field have opposite effects on the deformation of a soft dielectric, that is, the voltage makes the film thinner while the magnetic field makes the film thicker. Based on these results, along with the concept of a simple electric capacitor where capacitance decreases as thickness increases, we propose a simple design to increase the voltage between isolated charged films by applying an external magnetic field. A higher voltage can be exploited to do useful work—shown schematically in the form of powering a light-bulb (see Fig. 8). To make a rough estimate of how much energy can be harnessed in this case, we consider the simple model of a dielectric thin film with dimensions $L_1 = 10$ mm, $L_2 = 10$ mm and $L_3 = 1$ mm. The shear modulus of the soft material can be assumed to be of the order of $c = 10^6$ N m^{-2}, the electric permittivity $\varepsilon_0\hat{\varepsilon}_r = 4 \times 10^{-11}$ F m^{-1} and magnetic permittivity $\hat{\mu}_r = 5$. We assume a surface charge of density $q_0 = 1 \times 10^{-3}$ C m^{-2} at the upper surface and $-q_0$ at the lower surface of the thin film. Before applying the magnetic field, the capacitance of this dielectric capacitor is $C = \frac{Q}{V_0} = \frac{\varepsilon_0\hat{\varepsilon}_r L_1 L_2}{L_3}$. Note that the total charge on each surface, $Q = q_0 L_1 L_2$, is also conserved. Thus, the electric potential energy stored in the film

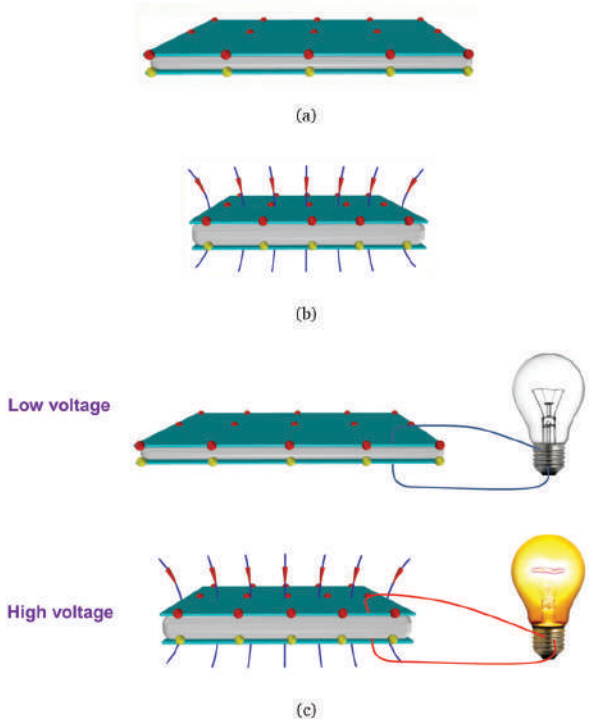

Fig. 8 Fixed total charges on the top and bottom layers of a dielectric film: (a) no magnetic field. The film thins down and expands its area which results in a large capacitance C. Since $C \sim Q/V$ and the charge Q is fixed, large C corresponds to low voltage V. (b) With external magnetic field. The thickness of the film increases whereas the area decreases. This results in a lower capacitance C. Lower C corresponds to large voltage V. (c) A higher voltage can power a connected device.

is $U_0 = \frac{1}{2}\frac{Q^2}{C} = \frac{1}{2}\frac{Q^2}{\varepsilon_0\hat{\varepsilon}_r}\frac{L_3}{L_1 L_2} \approx 1.25 \times 10^{-3}$ J. Normally, a magnetic field of 0.5 T (equivalent to 0.5×10^4 Oe) can deform the thin film and increase its thickness by about 10%. Substituting this 10% change in the thickness L_3, we can easily see that the electric potential energy stored in the capacitor can be increased by more than 20%. This amount of potential energy ($\sim 0.2U_0 = 250$ μJ) is due to the magnetic field. If the frequency of the magnetic field is 20 Hz, then the output power due to the magnetic field is ~ 250 μJ $\times$ 20 s^{-1} = 5 mW. This power is enough to power a single mini-LED. Of course, we have chosen a rather small piece of thin film as an example. In a realistic application, the output power can be further enhanced by increasing the size of the thin film, changing the magnetic permeability of the material and of course stacking multiple films together. In summary, the external magnetic field increases the voltage on the film and can be used for wireless energy harvesting.

6 Concluding remarks

In this paper, we have explored the magneto-electro-mechanical behavior and instability of soft materials under

the combined action of mechanical, electrical and magnetic loads. As long as the magnetic permeability of the soft matter is larger than that of vacuum, an emergent magnetoelectric effect appears due to the interaction of deformation and a pre-existing electric field. While this insight has been appreciated before,[19] our key emphasis in this paper is to explore the instability behavior of such a system. Our formulation is relatively general although, for illustrative results, we primarily focus on thin films and homogeneous deformation of an ideal neo-Hookean elastomer. Even for this simple case, the insights are rich. The presence of an external magnetic field gives us an important control variable to impact the equilibrium behavior of the dielectric thin film. In particular, pull-in instability can be significantly suppressed by applying an external magnetic field. As a result, the stability of the dielectric film is enhanced which allows it to sustain larger electric fields and mechanical loads. In contrast to the conventional interplay between mechanical and electrical fields, the interaction of three fields provides interesting opportunities to harness large deformation and instabilities of soft dielectrics and presents tantalizing prospects for wireless energy harvesting. Our work provides a simple basis to further explore magnetoelectric wireless energy harvesting devices. Further research on magneto-electro-mechanical instabilities could be elaborated to investigate the post-bifurcation analysis and the effects of the magnetic field on wrinkling, creasing, and cratering as well as other types of instabilities.

Conflicts of interest

There are no conflicts to declare.

Appendix A

We list the detailed derivations of the first variation (30) and the second variation (31) in the following.

A.1 Details of the first variation

Consider a smooth variation:

$$\delta\mathbf{v} = (\delta\lambda_2,\ \delta\lambda_3,\ \delta P,\ \delta M)^T \tag{A.63}$$

of the four generalized coordinates $\mathbf{v}$ in (23). Then the variation $\delta W^t(\mathbf{v})$ in (30) reads

$$\begin{aligned}\delta W^t(\mathbf{v}) = \delta W(\mathbf{v}) &- \varepsilon_0(\lambda_2\lambda_3\xi_{,X})\delta(\lambda_2\lambda_3\xi_{,X}) + \delta(\lambda_2\lambda_3\xi_{,X}P)\\ &+ \mu_0(\lambda_2\lambda_3\zeta_{,X}^{\text{self}})\delta(\lambda_2\lambda_3\zeta_{,X}^{\text{self}}) - \mu_0 h^{\text{e}}\delta M,\end{aligned} \tag{A.64}$$

where

$$\delta W(\mathbf{v}) = \frac{\partial W}{\partial\lambda_2}\delta\lambda_2 + \frac{\partial W}{\partial\lambda_3}\delta\lambda_3 + \frac{\partial W}{\partial P}\delta P + \frac{\partial W}{\partial M}\delta M, \tag{A.65a}$$

$$\delta(\lambda_2\lambda_3\xi_{,X}) = (\lambda_3\xi_{,X})\delta\lambda_2 + (\lambda_2\xi_{,X})\delta\lambda_3 + (\lambda_2\lambda_3)\delta\xi_{,X}, \tag{A.65b}$$

$$\delta(\lambda_2\lambda_3\xi_{,X}P) = (\lambda_3\xi_{,X}P)\delta\lambda_2 + (\lambda_2\xi_{,X}P)\delta\lambda_3 + (\lambda_2\lambda_3P)\delta\xi_{,X} + (\lambda_2\lambda_3\xi_{,X})\delta P, \tag{A.65c}$$

$$\delta(\lambda_2\lambda_3\zeta_{,X}^{\text{self}}) = (\lambda_3\zeta_{,X}^{\text{self}})\delta\lambda_2 + (\lambda_2\zeta_{,X}^{\text{self}})\delta\lambda_3 + (\lambda_2\lambda_3)\delta\zeta_{,X}^{\text{self}}. \tag{A.65d}$$

The terms related to the variation $\delta\xi_{,X}$ in (A.65b) and (A.65c) can be finally omitted by considering the Maxwell eqn (21) and the variation of the electric boundary conditions as well as integration by parts.

Similarly, the term related to the variation $\zeta_{,X}^{\text{self}}$ in (A.65d) can also be recast, that is,

$$\begin{aligned}\int_0^{L_1}\mu_0(\lambda_2\lambda_3\zeta_{,X}^{\text{self}})(\lambda_2\lambda_3)\delta\zeta_{,X}^{\text{self}}\mathrm{d}X &= \int_0^{L_1}\Big\{\mu_0(\lambda_2\lambda_3\zeta_{,X}^{\text{self}})[(\lambda_2\lambda_3)\delta\zeta_{,X}^{\text{self}} - \delta M]\\ &+\mu_0(\lambda_2\lambda_3\zeta_{,X}^{\text{self}})\delta M\Big\}\mathrm{d}X = \int_0^{L_1}\mu_0(\lambda_2\lambda_3\zeta_{,X}^{\text{self}})\delta M\mathrm{d}X.\end{aligned} \tag{A.66}$$

The first term on the second line disappears due to the zero variation of the Maxwell eqn (21) and the magnetic boundary condition with respect to the magnetization M.

Thus the first variation (30) can be written as

$$\frac{\delta F}{L_1L_2L_3} = \frac{1}{L_1}\int_0^{L_1}\left(\frac{\partial W^t}{\partial\mathbf{v}}\cdot\delta\mathbf{v}\right)\mathrm{d}X - s_2\delta\lambda_2 - s_3\delta\lambda_3 = 0. \tag{A.67}$$

Here the vector derivative has the component form

$$\frac{\partial W^t}{\partial\mathbf{v}} = \left(\frac{\partial W^t}{\partial\lambda_2}, \frac{\partial W^t}{\partial\lambda_3}, \frac{\partial W^t}{\partial P}, \frac{\partial W^t}{\partial M}\right)^T, \tag{A.68}$$

where the components are

$$\frac{\partial W^t}{\partial\lambda_2} = \frac{\partial W}{\partial\lambda_2} - \varepsilon_0\lambda_2\lambda_3^2\left(\xi_{,X}\right)^2 + \lambda_3\xi_{,X}P + \mu_0\lambda_2\lambda_3^2\left(\zeta_{,X}^{\text{self}}\right)^2, \tag{A.69a}$$

$$\frac{\partial W^t}{\partial\lambda_3} = \frac{\partial W}{\partial\lambda_3} - \varepsilon_0\lambda_2^2\lambda_3\left(\xi_{,X}\right)^2 + \lambda_2\xi_{,X}P + \mu_0\lambda_2^2\lambda_3\left(\zeta_{,X}^{\text{self}}\right)^2, \tag{A.69b}$$

$$\frac{\partial W^t}{\partial P} = \frac{\partial W}{\partial P} + \lambda_2\lambda_3\xi_{,X}, \tag{A.69c}$$

$$\frac{\partial W^t}{\partial M} = \frac{\partial W}{\partial M} + \mu_0(\lambda_2\lambda_3)^2\zeta_{,X}^{\text{self}}\left[\zeta_{,X}^{\text{self}}\right]_{,M} - \mu_0 h^{\text{e}}, \tag{A.69d}$$

$[\zeta_{,X}^{\text{self}}]_{,M}$ in (A.69d) is a coefficient related to the variations of the magnetization M and the self-magnetic field $\zeta_{,X}^{\text{self}}$ in (A.66).

A.2 Detailed second variation

Consider the integrand $\delta^2W^t(\mathbf{v})$ in (31).

$$\begin{aligned}\delta^2W^t(\mathbf{v}) &= \delta^2W(\mathbf{v}) - \frac{\varepsilon_0}{2}\delta^2\left[\left(\lambda_2\lambda_3\xi_{,X}\right)^2\right]\\ &+ \delta^2\left[\lambda_2\lambda_3\xi_{,X}P\right] + \frac{\mu_0}{2}\delta^2\left[\left(\lambda_2\lambda_3\zeta_{,X}^{\text{self}}\right)^2\right],\end{aligned} \tag{A.70}$$

where

$$\delta^2W(\mathbf{v}) = \delta\mathbf{v}\cdot\mathbb{H}^1\delta\mathbf{v}, \tag{A.71a}$$

$$\begin{aligned}\delta^2[(\lambda_2\lambda_3\xi_{,X})^2] &= 2(\lambda_3\xi_{,X})^2\delta\lambda_2^2 + 2(\lambda_2\xi_{,X})^2\delta\lambda_3^2 + 2(\lambda_2\lambda_3)^2\delta\xi_{,X}^2\\ &+ 8\lambda_2\lambda_3(\xi_{,X})^2\delta\lambda_2\delta\lambda_3 + 8\lambda_2\lambda_3^2\xi_{,X}\delta\lambda_2\delta\xi_{,X} + 8\lambda_2^2\lambda_3\xi_{,X}\delta\lambda_3\delta\xi_{,X},\end{aligned} \tag{A.71b}$$

$$\delta^2[\lambda_2\lambda_3\xi_{,X}P] = 2\{\xi_{,X}P\delta\lambda_2\delta\lambda_3 + \lambda_3 P\delta\lambda_2\delta\xi_{,X} + \lambda_3\xi_{,X}\delta\lambda_2\delta P + \lambda_2 P\delta\lambda_3\delta\xi_{,X} + \lambda_2\xi_{,X}\delta\lambda_3\delta P + \lambda_2\lambda_3\delta\xi_{,X}\delta P\}, \quad \text{(A.71c)}$$

$$\delta^2[(\lambda_2\lambda_3\zeta_X^{\text{self}})^2] = 2(\lambda_3\zeta_{,X}^{\text{self}})^2\delta{\lambda_2}^2 + 2(\lambda_2\zeta_{,X}^{\text{self}})^2\delta{\lambda_3}^2 + 2(\lambda_2\lambda_3)^2\delta(\zeta_{,X}^{\text{self}})^2 + 8\lambda_2\lambda_3(\zeta_{,X}^{\text{self}})^2\delta\lambda_2\delta\lambda_3 + 8\lambda_2{\lambda_3}^2\zeta_{,X}^{\text{self}}\delta\lambda_2\delta\zeta_{,X}^{\text{self}} + 8{\lambda_2}^2\lambda_3\zeta_{,X}^{\text{self}}\delta\lambda_3\delta\zeta_{,X}^{\text{self}}. \quad \text{(A.71d)}$$

Here $\mathbb{H}^1$ in (A.71a) is a fourth-order symmetric tensor

$$(\mathbb{H}^1)_{ij} = \left(\frac{\partial^2 W}{\partial v^2}\right)_{ij} = \frac{\partial^2 W}{\partial v_i \partial v_j}, \quad \text{(A.72)}$$

where $i, j = 1, 2, 3, 4$, and $\mathbf{v} = (\lambda_2, \lambda_3, P, M)^T$.

Combining (A.70)–(A.72), we can recast the second variation in a more compact form

$$\delta^2 W^t(\mathbf{v}) = \delta\mathbf{v}\cdot\mathbb{H}\delta\mathbf{v}, \quad \text{(A.73)}$$

where $\mathbb{H}$ is a fourth-order symmetric tensor

$$\mathbb{H} = \frac{\partial^2 W^t}{\partial \mathbf{v}^2} = \begin{pmatrix} \frac{\partial^2 W^t}{\partial {\lambda_2}^2} & \frac{\partial^2 W^t}{\partial\lambda_2\partial\lambda_3} & \frac{\partial^2 W^t}{\partial\lambda_2\partial P} & \frac{\partial^2 W^t}{\partial\lambda_2\partial M} \\ & \frac{\partial^2 W^t}{\partial {\lambda_3}^2} & \frac{\partial^2 W^t}{\partial\lambda_3\partial P} & \frac{\partial^2 W^t}{\partial\lambda_3\partial M} \\ & & \frac{\partial^2 W^t}{\partial P^2} & \frac{\partial^2 W^t}{\partial P\partial M} \\ & \text{Sym} & & \frac{\partial^2 W^t}{\partial M^2} \end{pmatrix} \quad \text{(A.74)}$$

with the entries

$$\frac{\partial^2 W^t}{\partial {\lambda_2}^2} = \frac{\partial^2 W}{\partial {\lambda_2}^2} - \varepsilon_0\left(\lambda_3{\xi_{,X}}^2\right) + \mu_0\left(\lambda_3\zeta_{,X}^{\text{self}}\right)^2, \quad \text{(A.75a)}$$

$$\frac{\partial^2 W^t}{\partial\lambda_2\partial\lambda_3} = \frac{\partial^2 W}{\partial\lambda_2\partial\lambda_3} - 2\varepsilon_0\lambda_2\lambda_3(\xi_{,X})^2 + P\xi_{,X} + 2\mu_0\lambda_2\lambda_3\left(\zeta_{,X}^{\text{self}}\right)^2, \quad \text{(A.75b)}$$

$$\frac{\partial^2 W^t}{\partial\lambda_2\partial P} = \frac{\partial^2 W}{\partial\lambda_2\partial P} + \lambda_3\xi_{,X}, \quad \text{(A.75c)}$$

$$\frac{\partial^2 W^t}{\partial\lambda_2\partial M} = \frac{\partial^2 W}{\partial\lambda_2\partial M} + 2\mu_0\lambda_2{\lambda_3}^2\zeta_{,X}^{\text{self}}\left[\zeta_{,X}^{\text{self}}\right]_{,M}, \quad \text{(A.75d)}$$

$$\frac{\partial^2 W^t}{\partial {\lambda_3}^2} = \frac{\partial^2 W}{\partial {\lambda_3}^2} - \varepsilon_0\left(\lambda_2\xi_{,X}\right)^2 + \mu_0\left(\lambda_2\zeta_{,X}^{\text{self}}\right)^2, \quad \text{(A.75e)}$$

$$\frac{\partial^2 W^t}{\partial\lambda_3\partial P} = \frac{\partial^2 W}{\partial\lambda_3\partial P} + \lambda_2\xi_{,X}, \quad \text{(A.75f)}$$

$$\frac{\partial^2 W^t}{\partial\lambda_3\partial M} = \frac{\partial^2 W}{\partial\lambda_3\partial M} + 2\mu_0{\lambda_2}^2\lambda_3\zeta_{,X}^{\text{self}}\left[\zeta_{,X}^{\text{self}}\right]_{,M}, \quad \text{(A.75g)}$$

$$\frac{\partial^2 W^t}{\partial P^2} = \frac{\partial^2 W}{\partial P^2}, \quad \text{(A.75h)}$$

$$\frac{\partial^2 W^t}{\partial P\partial M} = \frac{\partial^2 W}{\partial P\partial M}, \quad \text{(A.75i)}$$

$$\frac{\partial^2 W^t}{\partial M^2} = \frac{\partial^2 W}{\partial M^2} + \mu_0(\lambda_2\lambda_3)^2\left[\zeta_{,X}^{\text{self}}\right]_{,M}^2. \quad \text{(A.75j)}$$

Acknowledgements

The authors gratefully acknowledge support from the University of Houston M. D. Anderson Professorship and NSF grant CMMI-1463205. Q. D. gratefully acknowledges the support from NSFC-11672222.

References

1 N. Lu and D.-H. Kim, *Soft Robot.*, 2014, **1**, 53–62.
2 S. Shian, K. Bertoldi and D. R. Clarke, *Adv. Mater.*, 2015, **27**, 6814–6819.
3 J. A. Rogers, T. Someya and Y. Huang, *Science*, 2010, **327**, 1603–1607.
4 R. Shankar, T. K. Ghosh and R. J. Spontak, *Soft Matter*, 2007, **3**, 1116–1129.
5 M. Moscardo, X. Zhao, Z. Suo and Y. Lapusta, *J. Appl. Phys.*, 2008, **104**, 093503.
6 C. Keplinger, M. Kaltenbrunner, N. Arnold and S. Bauer, *Proc. Natl. Acad. Sci. U. S. A.*, 2010, **107**, 4505–4510.
7 S. J. A. Koh, X. Zhao and Z. Suo, *Appl. Phys. Lett.*, 2009, **94**, 262902.
8 J. Huang, S. Shian, Z. Suo and D. R. Clarke, *Adv. Funct. Mater.*, 2013, **23**, 5056–5061.
9 S. Bauer, S. Bauer-Gogonea, I. Graz, M. Kaltenbrunner, C. Keplinger and R. Schwödiauer, *Adv. Mater.*, 2014, **26**, 149–162.
10 Q. Deng, M. Kammoun, A. Erturk and P. Sharma, *Int. J. Solids Struct.*, 2014, **51**, 3218–3225.
11 S. Yang, X. Zhao and P. Sharma, *Soft Matter*, 2017, **13**, 4552–4558.
12 N. A. Hill, *Annu. Rev. Mater. Res.*, 2002, **32**, 1–37.
13 R. Ramesh and N. A. Spaldin, *Nat. Mater.*, 2007, **6**, 21.
14 W. Eerenstein, N. Mathur and J. F. Scott, *Nature*, 2006, **442**, 759.
15 J. Van Suchtelen, *Philips Res. Rep.*, 1972, **27**, 28–37.
16 M. Fiebig, *J. Phys. D: Appl. Phys.*, 2005, **38**, R123.
17 A. P. Pyatakov and A. K. Zvezdin, *Phys.-Usp.*, 2012, **55**, 557–581.
18 J. Velev, S. Jaswal and E. Tsymbal, *Philos. Trans. R. Soc., A*, 2011, **369**, 3069–3097.
19 L. Liu and P. Sharma, *Phys. Rev. E: Stat., Nonlinear, Soft Matter Phys.*, 2013, **88**, 040601.
20 Z. Alameh, Q. Deng, L. Liu and P. Sharma, *J. Mater. Res.*, 2015, **30**, 93–100.
21 S. Krichen, L. Liu and P. Sharma, *Phys. Rev. E*, 2017, **96**, 042404.
22 Y. Han, W. Hong and L. E. Faidley, *Int. J. Solids Struct.*, 2013, **50**, 2281–2288.
23 K. Stark and C. Garton, *Nature*, 1955, **176**, 1225–1226.
24 J.-S. Plante and S. Dubowsky, *Int. J. Solids Struct.*, 2006, **43**, 7727–7751.

25 X. Zhao and Z. Suo, *Appl. Phys. Lett.*, 2007, **91**, 061921.
26 Q. Wang, L. Zhang and X. Zhao, *Phys. Rev. Lett.*, 2011, **106**, 118301.
27 Q. Wang, Z. Suo and X. Zhao, *Nat. Commun.*, 2012, **3**, 1157.
28 Q. Wang and X. Zhao, *Phys. Rev. E: Stat., Nonlinear, Soft Matter Phys.*, 2013, **88**, 042403.
29 S. Yang, X. Zhao and P. Sharma, *J. Appl. Mech.*, 2017, **84**, 031008.
30 X. Zhao and Q. Wang, *Appl. Phys. Rev.*, 2014, **1**, 021304.
31 S. Kankanala and N. Triantafyllidis, *J. Mech. Phys. Solids*, 2004, **52**, 2869–2908.
32 K. Danas, S. Kankanala and N. Triantafyllidis, *J. Mech. Phys. Solids*, 2012, **60**, 120–138.
33 D. Ivaneyko, V. Toshchevikov, M. Saphiannikova and G. Heinrich, *Soft Matter*, 2014, **10**, 2213–2225.
34 L. Liu, *J. Mech. Phys. Solids*, 2014, **63**, 451–480.
35 L. Dorfmann and R. W. Ogden, *Proc. R. Soc. A*, 2017, **473**, 20170311.